ELSEVIER

International Journal of Mass Spectrometry 185/186/187 (1999) 795–812

International Journal of Mass Spectrometry

Mass spectrometric analysis of pentafluorobenzyl oxime derivatives of reactive biological aldehydes

F.-F. Hsu, S.L. Hazen[1], D. Giblin, J. Turk, J.W. Heinecke, M.L. Gross*

Mass Spectrometry Research Resource, Departments of Medicine, Chemistry, and Molecular Biology and Pharmacology, Washington University, St. Louis, MO 63110, USA

Received 13 July 1998; accepted 20 July 1998

Abstract

We recently demonstrated that a battery of reactive aldehydes can be generated by human neutrophils through the action of myeloperoxidase on α-amino acids. To determine the aldehydes, we formed the pentafluorobenzyloxime (PFBO) derivatives by reacting them with pentafluorobenzylhydroxylamine (PFBHA) and submitting the derivatives to gas chromatography electron-capture mass spectrometry (GC/EC/MS). Two geometric isomers are formed for each of the aldehydes, and they are separable by gas chromatography (GC) and exhibit distinguishable electron-capture (EC) mass spectra. Major fragment ions include $[M - HF]^{-\cdot}$, which probably has a six-membered ring formed via HF loss from the molecular radical anion. Subsequent decomposition of this intermediate yields other characteristic ions (e.g. those formed by elimination of NO and the anion of m/z 178). We proposed fragmentation pathways and mechanisms that are consistent with the data derived from collisionally-activated dissociations (CAD) coupled with tandem mass spectrometry, exact-mass measurements, studies of deuterium-labeled analogs, and calculations by PM3 semiemperical and ab initio methods. The generality of the structurally informative fragmentation pattern together with GC separation is the basis of a powerful means for the identification of reactive aldehydes in biological processes and the pathogenesis of disease. (Int J Mass Spectrom 185/186/187 (1999) 795–812) © 1999 Elsevier Science B.V.

Keywords: Aldehydes; Pentafluorobenzyl oxime; Mass spectrometry

1. Introduction

Reactive aldehydes have been implicated in a wide range of physiological processes [1, 2]. They may also contribute to the complications of diabetes mellitus, atherogenesis, alcoholic cirrhosis, and the aging process [1–4]. These biological effects are likely derived from the selective reactivity of the aldehyde with target molecules containing nucleophilic groups. For example, 4-hydroxy-2-nonenal (HNE), a cytotoxic decomposition product of lipid peroxidation, spontaneously forms Michael adducts with sulfhydryl, histidyl, and lysyl residues. Recent studies demonstrate that activated phagocytes oxidize virtually all of the common amino acids into reactive aldehydes by a pathway involving the generation of HOCl by myeloperoxidase (MPO) [5–9] [Eq. (1)]:

$$\mathrm{R{-}\underset{\displaystyle \mathrm{NH_2}}{\underset{|}{CH}}{-}CO_2H} \xrightarrow[H_2O_2,\ Cl^-]{MPO} \mathrm{RCHO} \qquad (1)$$

* Corresponding author.

[1] Present address: Dept. of Cell Biology, Cleveland Clinic Foundation, Cleveland, OH 44195.

Dedicated to Professor Michael T. Bowers on the occasion of his 60th birthday.

PII S1387-3806(98)14105-2

The amphipathic reactive aldehydes generated by myeloperoxidase may then modify critical molecular targets at sites of inflammation through formation of various covalent adducts. Thus, generation of aldehydes from amino acids represents a mechanism for phagocyte-mediated damage at sites of inflammation and vascular disease [5–9].

In previous gas chromatography/mass spectrometry (GC/MS) studies, volatile pentafluorobenzyloxime (PFBO) derivatives were prepared by reaction with the reagent pentafluorobenzylhydroxylamine (PFBHA) and used in the detection of short-chain α-hydroxyaldehydes [10] and aldehydes derived from lipid peroxidation [11,12]. High-energy tandem mass spectrometric studies of PFBO derivatives of ketosteroids [13,14] and of guneribone [15] were reported. Here we employed GC/MS, high-energy collisionally activated decomposition (CAD) by linked-scanning and tandem mass spectrometry (MS/MS), and exact-mass measurements in a systematic investigation of the electron-capture (EC) mass spectra of the PFBO derivatives of aldehydes derived from lipid peroxidation and oxidation of α-amino acids. We also analyzed the characteristic fragment ions of the PFBO derivatives of d_8-phenylacetaldehyde by the same methods to determine the fragmentation pathways and the nature of the fragment ions characteristic of this class of compounds. Furthermore, we performed theoretical calculations by semiempirical PM3 and ab initio methods for structural determination of the precursor, intermediate, and fragment ions, the calculation of the associated reaction energetics, and the assessment of mechanistic feasibility of the proposed fragmentation pathways.

2. Experimental

2.1. Aldehydes

Malondialdehyde (MDA) was prepared by acid hydrolysis of 1,1,3,3-tetramethoxypropane (Sigma Chemical Co., St. Louis, MO). Standard amino acids were oxidized to their respective aldehydes and purified by high-performance liquid chromatography (HPLC) as described previously [9]. In brief, amino acids (100 nmol) were incubated individually in gas-tight vials (1 mL) in the presence of myeloperoxidase (20 pmol), H_2O_2 (100 nmol), and NaCl (100 μmol) in sodium phosphate buffer (50 mM, pH 7.0) at 37 °C for 30 min. Doug Spitz of Washington University School of Medicine generously provided the 4-hydroxy-2-nonenal (HNE). The d_8-phenylacetaldehyde was purchased as the amino acid, DL-phenyl-d_5-alanine-2,3,3-d_3, from Isotec, Inc. (Miamisburg, OH) and converted to the aldehyde by the procedure described in this section. Pentafluorobenzylhydroxylamine (PFBHA) was obtained from Aldrich Chemical (St. Louis).

2.2. PFBO derivatives of aldehydes

Aldehydes dissolved in phosphate-buffered saline (100 mM NaCl, 50 mM sodium phosphate, pH 7.0) were cooled to 0 °C, and the derivatizing reagent PFBHA was added in twofold molar excess relative to the original total amino acid concentration. Sodium hydroxide (final concentration 1 M) was then added and the vials were capped, heated to 65 °C for 1 h, and cooled to 0 °C. Extraction was performed with an equal volume (1 mL) of ethyl acetate, and the residual aqueous solution was acidified to pH 2 with concentrated HCl and again extracted with another 1 mL of ethyl acetate. The extracts were combined and stored in gas-tight vials until analysis.

2.3. Mass spectrometry

EC mass spectra were acquired on a Hewlett-Packard 5988A GC/MS instrument coupled with a Teknivent Vector I data system. Mixtures of the PFBO derivative of amino-acid oxidation products were analyzed by GC on a Restek RTX-200 column (15 m, 0.33 mm id, 1 μm film thickness) threaded into the ion source of the mass spectrometer. The initial GC oven temperature of 70 °C was increased to 150 °C at a rate of 10 °C/min, and then raised to a final temperature of 280 °C at a rate of 20 °C/min. Both high-resolution (10 000 resolving power) exact-mass measurements, and linked-scanning experiments

were performed on a VG (Micromass, formerly VG, Manchester, England) ZAB-SE double-focusing instrument equipped with an Opus 3.2 data system. The linked-scanning experiments gave information on CAD in the first field-free region. The CAD tandem mass spectrometric experiments were performed on a VG ZAB-T four sector (BEBE) instrument also equipped with an Opus 3.2 data system; fragmentation was induced in a collision cell between the two double-focusing BE sections so that both precursor and fragment ions could be selected and analyzed with greater resolving power than that afforded by a single double-focusing BE instrument. Ion-source temperatures of the VG sector instruments were maintained at 150 °C, and methane was the moderating gas for EC. Perfluorokerosene was used as the internal standard for high-resolution exact-mass measurements.

2.4. Theoretical calculations

To elucidate the structures of the molecular ion and characteristic fragment ions, we undertook a program of molecular modeling at the semiempirical PM3 level of parameterization [16, 17] and by ab initio methods to determine the most likely structures corresponding to the molecular formulas and reasonable reaction pathways. The semiempirical algorithm with the PM3 Hamiltonian (hereafter referred to as the PM3 method) has a good record for determining structures, but the calculated heats of formation are considered semiquantitative. Even with this limitation, the geometric and thermochemical results of the method can be used to guide the selection of likely mechanisms and related structures as encountered in breakdown schemes. The advantage of the PM3 method is its ability to handle much larger systems than is practical for ab initio procedures. The PM3 method was chosen for this study because of the sizes of the structures involved. In addition, we found that the PM3 method gave results that parallel ab initio calculations on certain fragments (see below), a correspondence that was much closer than that produced by the semiempirical AM1 level of parametrization.

Minima corresponding to the molecular anions, postulated intermediates, and characteristic fragments were located by geometric optimization. The potential energy surfaces for the syn and anti isomers of the PFBO derivatives of both benzaldehyde and phenylacetaldehyde were investigated by using the PM3 method. Heats of formation for all minima were calculated and employed in screening candidates for likely intermediates in the fragmentation processes because differences in heats of formation of the intermediates must conform to the range of energies available from the EC ionization process. In addition, reaction trajectories were calculated by the PM3 method, and the results were employed to locate transition states for some of the proposed reaction steps by eigenmode following. All minima and transition states were validated by performing vibrational analyses on the optimized geometries and checking the calculated Hessian matrices for the correct number of negative eigenvalues, either none or one, respectively. All heats of formation were calculated to standard conditions (temperature, 298.15 K, and pressure, 1 atm).

The PM3 method employed in this study is part of the Spartan v5.0 package (Wavefunction, Inc.) and was running on a Silicon Graphics Indigo II workstation. Furthermore, it will be assumed that all theoretical calculations in this study were performed by the PM3 method unless noted otherwise. The ab initio calculations were performed by using the GAUSSIAN 94 suite of programs [18, 19] (Gaussian, Inc.) running on a Silicon Graphics Power Challenge workstation.

Ab initio methods were used to optimize geometries and calculate energies for the further characterization of fragments produced by single-bond cleavages (see Scheme 1). Geometries were optimized at the Hartree–Fock level (HF) with the 6-31+G(d) basis set, which provides diffuse and polarization orbitals on the nonhydrogen atoms to account for radical and/or anionic character of the fragments and precursors. Vibrational analyses were performed on the optimized geometries at the same level of theory, and thermal-energy corrections to attain standard conditions were calculated from scaled zero-point energies and fundamental vibrational frequencies [20]. The thermal-energy corrections were added to the calculated energies of the various species. In addition, the vibrational analyses were used to vali-

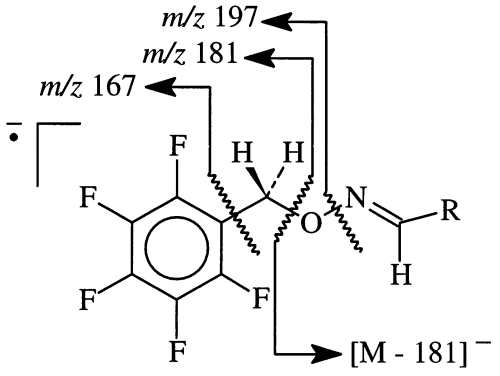

Scheme 1. Common fragment ions derived by single-bond cleavages of the radical anions of the PFBO derivatives of aldehydes.

date all optimized geometries as minima, i.e. no imaginary frequencies were found. The final stage of refinement, which involved geometric optimization and energy calculation for each species, was performed by using Becke's hybrid functional, B3LYP [21], with the same basis set, 6-31+G(d).

Relative enthalpies of the simple-cleavage reactions were calculated from the heats of formation of the reaction components obtained from calculations by the PM3 method or from the corrected energies derived from ab initio calculations with the addition of RT to account for differences in the number of products produced by some of the cleavages. The single-bond cleavage that produces 2,3,4,5,6-pentafluorobenzyl anion was used to set the zero point on the relative enthalpy scale for the cleavage reactions. The differences in the energetics of the fragmentation processes that give rise to the simple cleavage products serve to put limits upon the range of energies available from the electron-capture process; the available energy must be sufficient to drive the fragmentation and rearrangement reactions.

The same ab initio procedures were used to calculate the corrected energies associated with various possible structures for the fragment ion of m/z 178. The differences in energy, identical to differences in heats of formation in this case, allowed us to propose likely reaction mechanisms and to postulate the structure of this ion.

3. Results and discussion

In Table 1, we present the formulas and likely structures of malondialdehyde (MDA), HNE, which are two products formed from lipid peroxidation, acrolein and benzaldehyde, which are two known toxic aldehydes, and aldehydes generated by myeloperoxidase-catalyzed (MPO-catalyzed) oxidation of 13 naturally occurring α-amino acids.

Typically, two geometric isomers (syn and anti, see below) of PFBO-derivatives of each aldehyde are formed in the derivatization reaction [Eq. (2)].

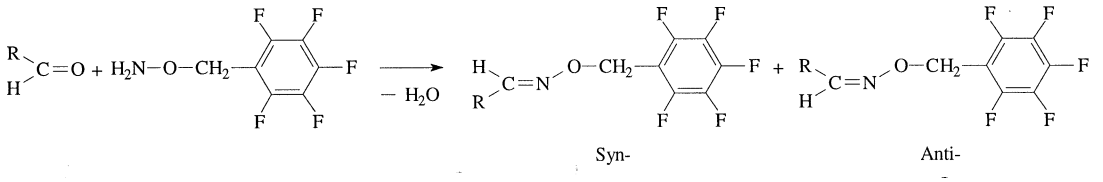

(2)

These isomers are usually separable by GC [15] as illustrated by the ion chromatograms of the PFBO derivative of HNE shown in Fig. 1. Typically, the anti-isomer elutes before the syn isomer [11]. The GC retention times and the abundances of molecular and characteristic fragments ions represented in the EC mass spectra of the 17 compounds included in this study are summarized in Table 1. (We have applied the conventional use of syn and anti designations for the configuration of oximes [22] to the stereoisomers of the PFBO derivatives [11].)

When the syn and anti isomers of the PFBO aldehydes were separable by GC, we found that the isomers exhibited distinguishable EC mass spectra (see Tables 1 and 2 as well as Figs. 2 and 3). Furthermore, the patterns of abundance for the $M^{-\cdot}$,

Table 1
NCI mass spectra of PFBO derivatives of aldehydes, the relative abundances of characteristic ions

Parent amino acid		Aldehyde (R-CHO)	r.t. (min.)	$M^{-\cdot}$	$[M-HF]^{-\cdot}$	$[M-HF-HCN]^{-\cdot}$	$[M-HF-NO]^{-\cdot}$	$[M-181]^{-\cdot}$	*m/z* 204	*m/z* 197	*m/z* 196	*m/z* 181	*m/z* 178	*m/z* 167
Gly		H−	3.13	4.2 (225)	9.5 (205)	** (178)	29 (175)	nd (44)	nd	10	4	100	80	2.7
Ala	anti	CH_3−	4.24	0.2 (239)	8.9 (219)	nd (192)	16 (189)	nd (58)	nd	12	31	100	54	8.6
	syn		4.38	0.6	9.6	4	3.9		nd	14	13	100	60	5
Val	anti	$(CH_3)_2CH$−	5.72	0.1 (267)	7 (247)	nd (220)	6.3 (217)	nd (86)	6.1	5	35	89	100	6
	syn		5.80	13	2.6	5.3	nd		nd	19	4	100	41	3.7
Ile	anti	$CH_3CH_2C(CH_3)H$−	6.78	0.3 (281)	4 (261)	nd (234)	3.3 (231)	0.1 (100)	3.4	13	25	85	100	0.1
	syn		6.82	4.3	3.7	2.6	0.7		0.7	19	21	100	77	1.7
Leu	anti	$CH_3(CH_2)_3$−	6.98	nd (281)	13 (261)	nd (234)	14 (231)	nd (100)	2.5	9.8	31	46	100	2.7
	syn		7.16	4.7	23	8.1	4.7		0.4	22	41	100	90	7.5
Ser	anti	$HOCH_2$−	8.17	nd (255)	1.2 (235)	nd (208)	18 (205)	0.4 (74)	76	10	53	9.6	100	7.2
	syn		8.31	4.7	32	nd	nd	50	20	3	10	0.1	100	nd
Thr	anti	$CH_3C(OH)H$−	9.42	nd (269)	37 (249)	nd (222)	1.7 (219)	0.2 (88)	13	26	38	nd	100	2.5
	syn		9.56	0.3	12	nd	3.7	9	3	7.7	82	14	100	11
Asp	anti	$HOOCCH_2$−	9.53	nd (283)	57 (263)	0.3 (236)	0.7 (233)	1.8 (102)	5.8	24	1.2	2.1	100	nd
	syn		9.69	nd	17	0.2	0.3	67	2.3	nd	0.4	1.3	100	0.7
Lys†		$NH_2(CH_2)_4$−	10.60	nd (296)	21 (276)	nd (249)	6.0 (246)	nd (115)	nd	6.7	1.3	14	100	5.9
Phe	anti	$C_6H_5CH_2$−	11.15	nd (315)	1.0 (295)	0.6 (268)	1.0 (265)	0.2 (134)	57	8	8	22	100	1
	syn		11.26	1.3	34	47	0.2	0.6	26	26	0.7	15	100	nd
Glu†		$HOOC(CH_2)_2$−	11.22	2 (297)	1.5 (277)	nd (250)	0.1 (247)	100 (116)	nd	nd	5.6	0.5	15	nd
Tyr	anti	$HO(C_6H_4)CH_2$−	13.10	0.8 (331)	100 (311)	nd (284)	1.0 (281)	0.7 (150)	0.6	nd	nd	nd	100	nd
	syn		13.21		100	2.5	nd	0.5	nd	2	16	5	11	6
Trp	anti	$C_8H_6NCH_2$−	14.62	0.3 (354)	100 (334)	nd (307)	nd (304)	20 (171)	0.2	4	48	8.8	9	3
	syn		14.76	nd	100	nd	0.1	6.4	nd	3	35	6	4.4	2.7
*Acrolein	anti	CH_2=CH−	5.35	0.4 (251)	82 (231)	0.8 (204)	100 (201)	2 (70)	0.8	3	20	10	23	12
	syn		5.64	9	61	2	87		2	11	50	100	94	16
*MDA		$CH_2(CHO)$−	13.39	nd (462)	19 (442)	47 (415)	0.5 (412)	54 (281)	100	7.5	25	18	41	8.1
			13.42	nd	nd	nd	0.6	0.3	100	0.1	2.3	6.3	17	1.3
			13.46	nd	20	34	0.5	100	85	7.4	8	5.6	67	9.6
*Benzaldehyde	anti	C_6H_5−	10.10	2.7 (301)	50 (281)	nd (254)	72 (251)	40 (120)	0.2	6.5	46	100	63	61
	syn		10.90	nd	85	nd	97	64	0.3	4.9	43	6.5	20	100
*4-HNE	anti	$CH_3(CH_2)_4CHOHCH$=CH−	12.89	0.8 (351)	63 (331)	0.6 (304)	15 (301)	10 (170)	1	21	100	3	23	8.6
	syn		12.91	2.2	100	1.5	40	41	2	8	82	2	12	22

nd = not detected (relative abundance <0.1%); †syn and anti isomers not baseline resolved; *standard aldehyde; **interference overlap with *m/z* 178.
Data for the $[M - X]^-$ are reported as: relative abundance (*m/z*).
Some data presented in this table were previously published [9] albeit with reversed syn and anti designations [11].

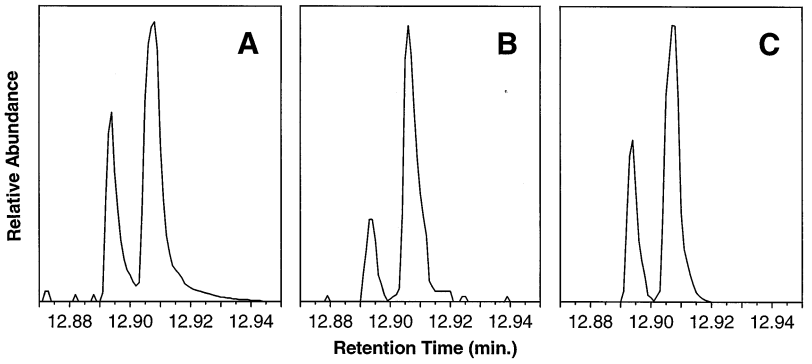

Fig. 1. The EC/GC mass chromatogram of the PFBO derivative of HNE. (A) TIC; (B) trace of the m/z 351 ion, $M^{-\cdot}$; (C) trace of the m/z 331 ion, $[M-HF]^{-\cdot}$.

$[M - HF - HCN]^{-\cdot}$, and $[M - 181]^{-\cdot}$ ions favor the later eluting component, whereas that for the $[M - HF - R]^{-}$ ion tracks the earlier eluting component (see Table 2), which indicates that the early/late groupings form consistent classes that are tenable with the previous report that anti-isomers elute before syn isomers [11]. In addition, fragment ions that strongly track the geometric isomers must be definitely linked through intermediates that retain the stereochemistry of the original isomers.

Table 2
Summary of trends in ion abundances from Table 1

	Abundance ratios	
Fragment Ion	syn	anti
$M^{-\cdot}$	+	
$[M - HF]^{-\cdot}$		
$[M - HF - HCN]^{-\cdot}$	+	
$[M - HF - NO]^{-}$		
$[M - 181]^{-}$ [b]	*w*	
m/z 204 = $[M - HF - R]^{-}$ [a]		*w*
m/z 197 [b]		
m/z 196		
m/z 181 [b]		
m/z 178 = $[M - HF - RCN]^{-\cdot}$ [a]		
m/z 167 [b]		

Mean fractional abundances of each species of ion for the syn and anti isomers, A_{syn} and A_{anti}, were calculated from the fractional abundances for the ions represented in the EC mass spectra of the PFBO derivatives of acrolein, benzaldehyde, and the aldehydes derived by MPO oxidation of the amino acids: Ala, Val, Ile, Leu, Ser, Thr, Asp, Phe, Tyr, and Trp. The syn and anti abundance ratios designate the ratios A_{syn}/A_{anti} and A_{anti}/A_{syn}. A "+" in a column indicates that an abundance ratio exceeds 5.0, a "*w*" denotes a ratio in the range 1.5–5.0, and a blank entry indicates a ratio less than 1.5.

[a] R refers to base group in the aldehyde R–CHO.

[b] Fragments ions from simple cleavages.

To account for the fragmentation patterns as presented in Tables 1 and 2, we propose that the major fragment ions of the radical anions of the PFBO-aldehydes fall into two classes. First, fragment ions arise from single-bond cleavages of the molecular anion $M^{-\cdot}$ (see Scheme 1). The fractional abundances of these fragments are not expected to track strongly either of the isomers. Second, fragment ions arise through fragmentation of various rearrangement intermediates (see Schemes 2 and 3).

3.1. Simple fragmentations

The relative enthalpies of the various simple cleavages of PFBO-benzaldehyde (see Table 3) anions as calculated by the PM3 and ab initio methods (see Sec. 2.4, Experimental) correlate with those single-bond cleavages actually observed (see Scheme 1, Table 3). All simple cleavages are endothermic as calculated by the PM3 method, and the cleavage producing the 2,3,4,5,6-pentafluorobenzyl anion is used as the zero on the enthalpic scale for the simple cleavages. The relative enthalpies of the observed cleavages of the PFBO-benzaldehyde anion are clustered in the range of −12.6 to 0.0 kcal mol^{-1} by ab initio methods (0.0 to 18.5 kcal mol^{-1} by PM3), whereas the relative enthalpies for other cleavages that do not occur range

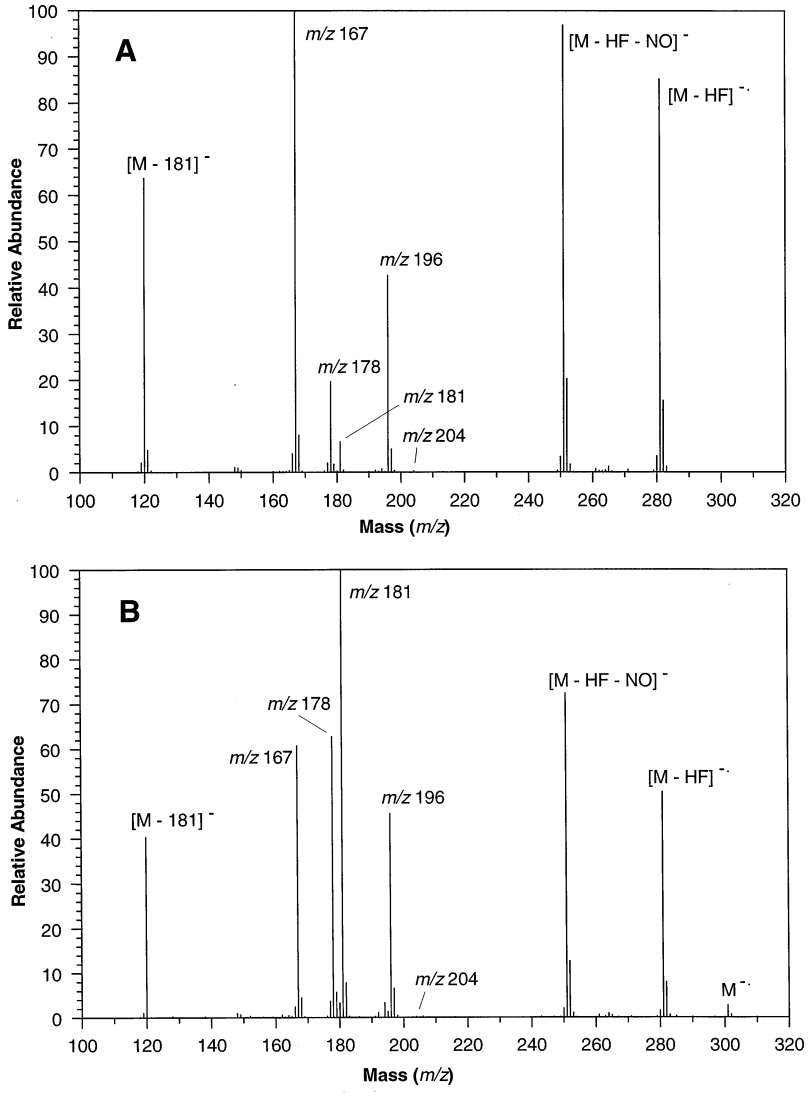

Fig. 2. The EC mass spectra of the syn (A) and anti (B) isomers of the PFBO derivatives of benzaldehyde.

from 25.6 to 52.2 kcal mol^{-1} (26.4 to 51.1 kcal mol^{-1} by PM3—see Table 3). The neutral precursor of the syn-PFBO-benzaldehyde anion has a relative heat of formation of -16.3 kcal mol^{-1} by PM3. For the PFBO-phenylacetaldehyde anion, the heat of formation of the precursor is -17.6 kcal mol^{-1}, and the observed cleavages require 0.0 to 16.9 kcal mol^{-1} additional energy whereas the cleavages that do not occur require 28.5 to 53.2 kcal mol^{-1} (by the PM3 method). The simple cleavages that do not occur require more energy to initiate than the cleavages that are observed.

In the absence of any activation barrier, the difference between the heat of reaction for a fragmentation and the heat of formation of the precursor represents a lower bound in the energy required to drive that cleavage, energy that must come from the electron-capture ionization and residual thermal energy of the neutral. Similarly, the energetics of the cleavages that do not occur, plus the associated activation barriers

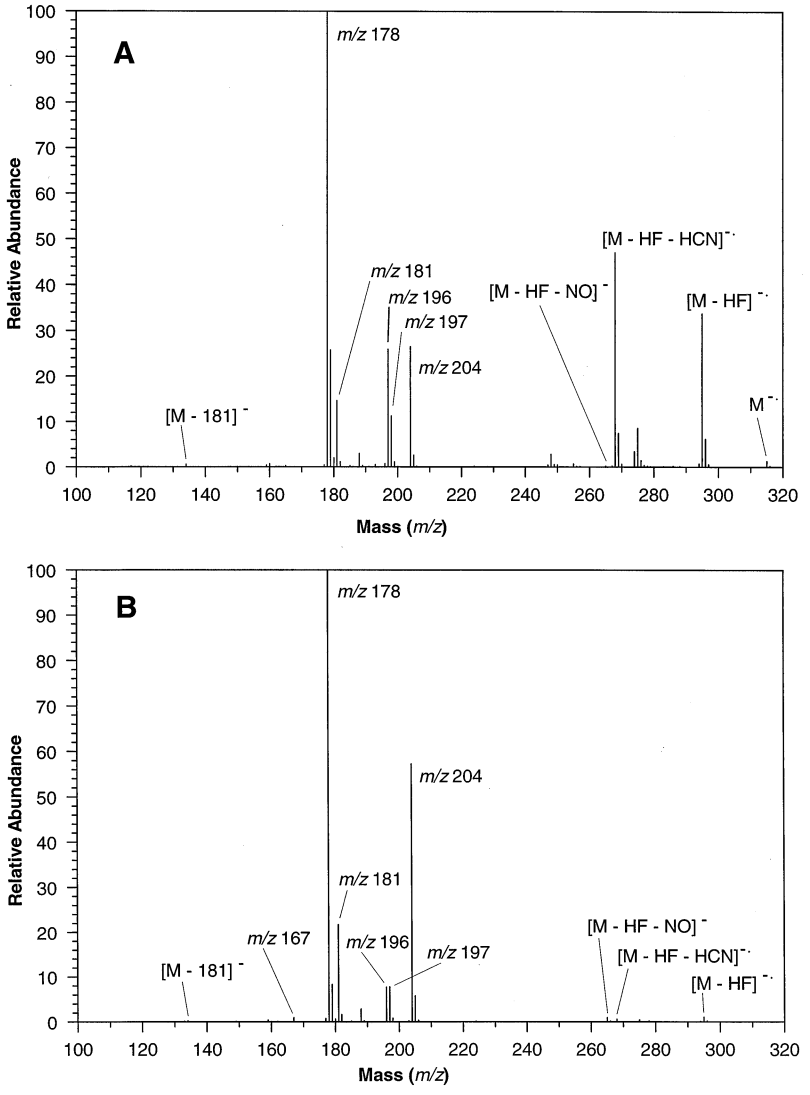

Fig. 3. The EC mass spectra of the syn (A) and anti (B) isomers of the PFBO derivatives of phenylacetaldehyde.

and kinetic shifts, place upper limits on the energy available from the ionization event. The energetics for simple cleavages of both anions are very similar and point to a maximum energy available in the range of 40 to 60 kcal mol^{-1}.

The fragmentations that give rise to the *m*/*z* 196 ion and the unobserved $[M-196]^-$ from both PFBO-benzaldehyde and PFBO-phenylacetaldehyde anions are energetically more favorable than the observed simple cleavages and are exothermic with respect to the precursors as calculated by PM3. That the *m*/*z* 196 ion does not dominate the EC mass spectra and the $[M-196]^-$ ion is not observed strongly indicate that the *m*/*z* 196 ion arises by another mechanism other than H· transfer accompanying a single bond cleavage (see Scheme 2 and later discussion).

The $[M-181]^-$ ion that is observed in the EC mass spectra of the PFBO derivatives of several of the compounds listed in Table 1 may result from C–O bond cleavage as depicted in Scheme 1. The $[M-181]^-$ fragment ion is not abundant from the PFBO-derivatives of aldehydes derived from the ox-

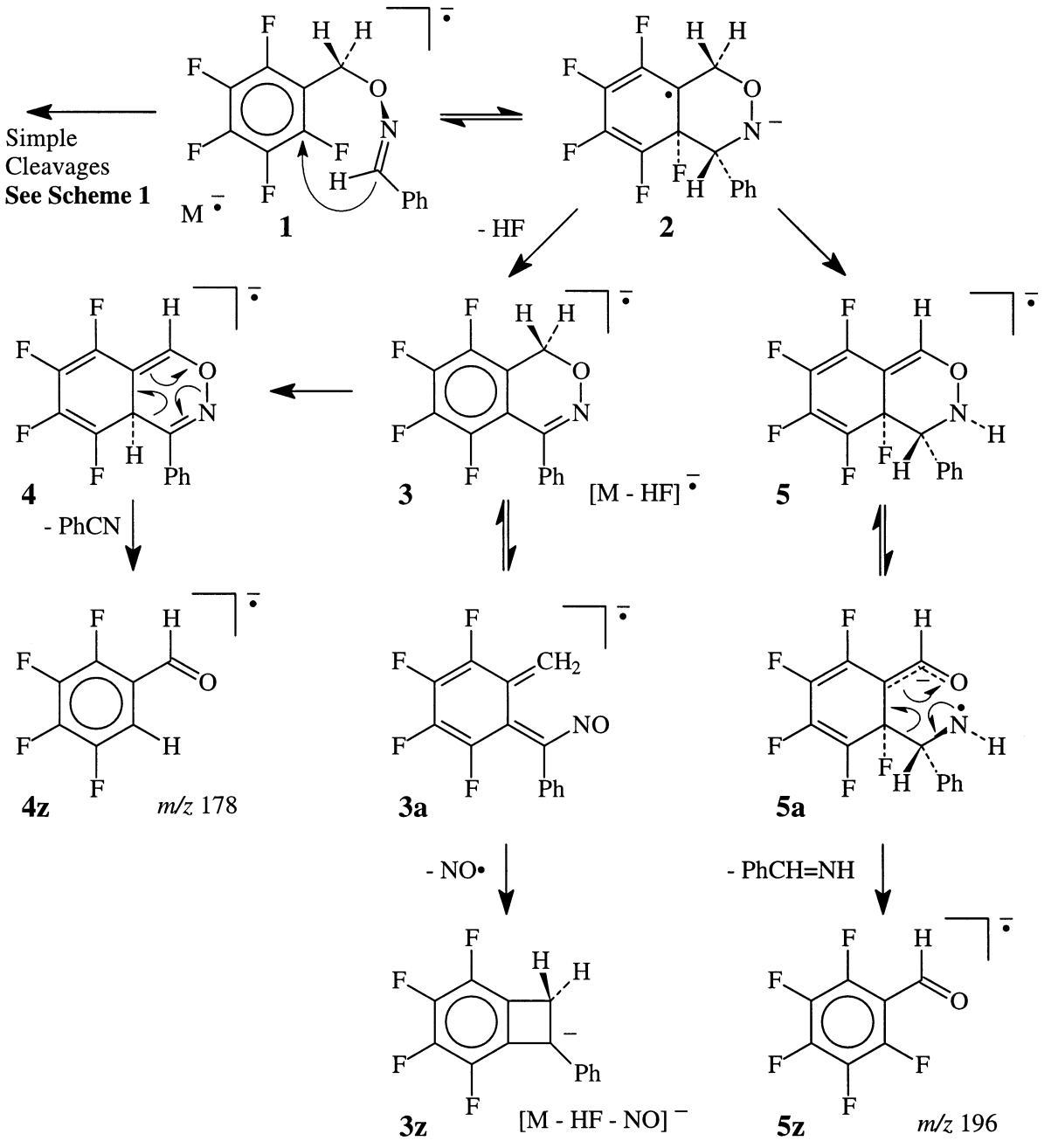

Scheme 2. Proposed fragmentation pathways of *syn*-PFBO-benzaldehyde radical anion. The pathways are common to all radical anions of the anti and syn PFBO derivatives of the aldehydes in this study.

idation of aliphatic amino acids (e.g. Gly, Ala, Val, or Leu), but it is formed more abundantly by the fragmentation of the PFBO-derivatives of benzaldehyde, MDA, and of aldehydes derived from the oxidation of amino acids with hydroxylated (e.g. Ser or Thr) or acidic (e.g. Glu or Asp) side chains. Such patterns of occurrence suggest that the dispersal of negative charge either onto hydroxy and carboxylate functions

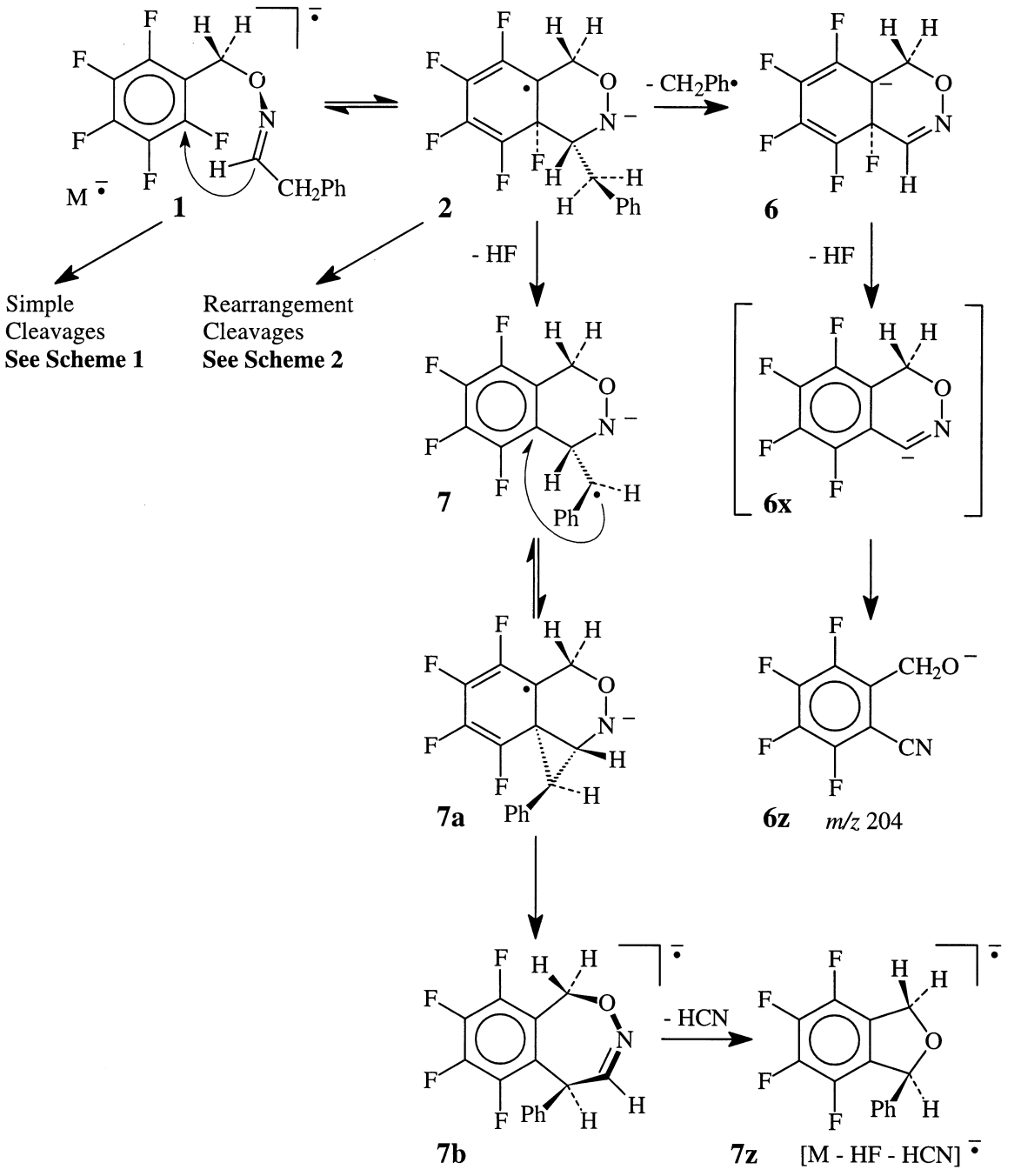

Scheme 3. Proposed fragmentation pathways of the *syn*-PFBO-phenylacetaldehyde radical anion. The additional pathway leading to product formed by loss of HCN pertains to derivatives of aldehydes that have α-hydrogens.

Table 3
Calculated relative energies of simple cleavages of the syn PFBO derivatives of benzaldehyde and phenylacetaldehyde

Potential fragment pairs (simple cleavages)			Calculated relative enthalpies (kcal mol^{-1})			
			R = C_6H_5-		R = $C_6H_5CH_2-$	Observed in spectra?
Aldehyde (R–CHO) end	PFBO end	*m/z*	PM3	Ab initio	PM3	
R–CHN$^{\cdot}$ + HCHO[a]	Pentafluorophenyl anion	167	18.5	−1.7	16.9	Yes
syn-R–CHNO$^{\cdot}$	Pentafluorophenyl-CH_2^-	181	0.0	0.0	0.0	Yes
syn-R–CHNO$^-$	Pentafluorophenyl-$CH_2^{\cdot}$	[M − 181]	2.7	−2.4	11.6	Yes
R–CHN$^{\cdot}$	Pentafluorophenyl-CH_2O^-	197	3.7	−12.6	2.1	Yes
R–CHN$^-$ + HCHO[a]	Pentafluorophenyl radical	[M − 197]	51.1	52.2	53.2	No
R–CHN$^-$	Pentafluorophenyl-$CH_2O^{\cdot}$	[M − 197]	26.4	25.6	28.5	No
R–CHNH	Pentafluorophenyl-CHO$^-$[b]	196	−58.1	−48.3	−59.3	Yes
R–CHNH$^-$	Pentafluorophenyl-CHO[b]	[M − 196]	−25.7	−19.4	−12.3	No
Precursor: *syn*-PFBO-benzaldehyde anion		301	−16.3			Yes (<0.1%)
Precursor: *syn*-PFBO-phenylacetaldehyde anion		315			−17.6	Yes

The relative enthalpies were calculated as the difference in enthalpies of reaction between a given fragmentation pathway and that which produces pentafluorophenyl-CH_2^- (2,3,4,5,6-pentafluorobenzyl anion), a commonly observed cleavage. The enthalpy of formation of the PFBO-benzaldehyde anion was not calculated by ab initio methods. The semiempirical PM3 and ab initio calculations were performed as described in Sec. 2 (Experimental) and the results presented are for the most stable conformations only.

[a]These fragmentations are expected to involve the concurrent fragmentation of the unstable intermediates, *syn*-R-$CHNOCH_2^{\cdot}$ and *syn*-R-$CHNOCH_2^-$, to R-CHN$^{\cdot}$ and R-CHN$^-$, respectively, and HCHO. The intermediates, *syn*-R-$CHNOCH_2^{\cdot}$ and *syn*-R-$CHNOCH_2^-$, are less stable than their respective fragments by 24.3 and 8.9 kcal mol^{-1} for R = C_6H_5- and 24.1 and 8.6 kcal mol^{-1} for R = $C_6H_5CH_2-$, as calculated by the PM3 method. The loss of HCHO likely proceeds readily without rearrangement, since reaction path calculations by PM3 yield maximum activation enthalpies of 2.9 and 2.1 kcal mol^{-1} for loss of HCHO from the radical and anion, respectively, for R = C_6H_5-.

[b]The fragmentation pathways that yield the pentafluorophenyl-CHO anion and neutral (radical anion and neutral 2,3,4,5,6-pentafluorobenzaldehyde) have been included since we initially thought these may arise from a single bond fragmentation accompanied by H$^{\cdot}$ shift.

or by conjugation into a phenyl ring aids the formation of this ion.

3.2. Rearrangement fragmentations

In Scheme 2, we present structures and mechanisms that are common to all PFBO-aldehydes as illustrated by starting with the PFBO-benzaldehyde anion. In Scheme 3, we present other mechanisms and related structures starting with the PFBO-phenylacetaldehyde anion, including the route leading to the product formed by the elimination of HCN, which only occurs when there are α-hydrogens on the parent aldehyde. The heats of formation for all species featured in Scheme 2 were calculated by the PM3 method (Table 4). For each intermediate or product ion, the heats of reaction are presented in two ways: the overall heat of reaction (Table 4) for the formation of that intermediate starting from the initial radical anion, **1**, and the stepwise heat of reaction (Table 4) for the preceding step that produced that intermediate. The intermediates presented in Schemes 2 and 3 were selected such that the mechanistic steps are structurally and energetically feasible, given the constraints implicated by the energetic requirements of the single-bond cleavages, and conform to known modes of isomerization and fragmentation of anions. (Schemes 2 and 3 are drawn illustrating the syn isomers.)

We analyzed trends in the abundances of the various ionic fragments presented in Table 1 by calculating the average fractional abundance of each type of ion in Table 1 with respect to the syn and antiisomers by using the fractional abundances of the ions produced in the EC mass spectra of each PFBO-aldehyde isomer for those PFBO-aldehydes where both syn and anti-isomers were available. We used the average fractional abundances of the syn and anti-isomers, A_{syn} and A_{anti}, respectively, to calculate the production ratios A_{syn}/A_{anti} and A_{anti}/A_{syn} for each type of ion. We found that the ratios fall into three

Table 4
Calculated energies of rearrangement fragmentations of the radical anions of the PFBO derivatives of benzaldehyde and phenylacetaldehyde (see Schemes 2 and 3)

Species number	Fragmentation class	*m/z*	Heat of formation (kcal mol^{-1})	Heat of reaction, overall (kcal mol^{-1})	Heat of reaction, stepwise (kcal mol^{-1})
syn-PFBO-benzaldehyde radical anion (R = C_6H_5-)					
1	$M^{-\cdot}$	301	−189.1	0.0	
2	$M^{-\cdot}$	301	−181.3	7.9	7.9
3	$[M-HF]^{-\cdot}$	281	−149.2	−22.8	−30.7
3a	$[M-HF]^{-\cdot}$	281	−135.2	−8.8	14.0
3z	$[M-HF-NO]^-$	251	−125.8	15.3	24.2
4	$[M-HF]^{-\cdot}$	281	−129.6	−3.2	19.6
4z	$[M-HF-RCN]^{-\cdot}$	178	−228.4	−43.6	−40.4
5	$M^{-\cdot}$	301	−189.7	−0.6	−8.5
5a	$M^{-\cdot}$	301	−215.4	−26.3	−25.7
5z	$[M-RCH=NH]^{-\cdot}$	196	−273.4	−41.8	−15.5
anti-PFBO-benzaldehyde radical anion (R = C_6H_5-)					
1	$M^{-\cdot}$	301	−188.7	0.0	
2	$M^{-\cdot}$	301	−182.4	6.3	6.3
3	$[M-HF]^{-\cdot}$	281	−212.0	−23.3	−29.6
syn-PFBO-phenylacetaldehyde radical anion (R = $C_6H_5CH_2-$)					
1	$M^{-\cdot}$	315	−194.0	0.0	
2	$M^{-\cdot}$	315	−190.4	3.6	3.6
3	$[M-HF]^{-\cdot}$	295	−154.8	−23.5	−27.1
3a	$[M-HF]^{-\cdot}$	295	−138.8	−7.5	16.0
3z	$[M-HF-NO]^-$	265	−121.8	24.1	31.6
4	$[M-HF]^{-\cdot}$	295	−136.9	−5.7	17.8
4z	$[M-HF-RCN]^{-\cdot}$	178	−228.4	−45.1	−39.4
5	$M^{-\cdot}$	315	−196.7	−2.7	−6.3
5a	$M^{-\cdot}$	315	−221.1	−27.2	−24.5
5z	$[M-RCH=NH]^{-\cdot}$	196	−273.4	−41.7	−14.5
6	$[M-R]^-$	224	−216.4	17.2	13.6
6z	$[M-R-HF]^-$	204	−165.9	4.9	−12.3
7	$[M-HF]^{-\cdot}$	295	−117.4	13.8	10.2
7a	$[M-HF]^{-\cdot}$	295	−112.8	18.5	4.7
7b	$[M-HF]^{-\cdot}$	295	−134.2	−2.9	−21.4
7z	$[M-HF-HCN]^{-\cdot}$	268	−192.0	−27.8	−24.9
anti-PFBO-phenylacetaldehyde radical anion (R = $C_6H_5CH_2-$)					
1	$M^{-\cdot}$	315	−195.5	0.0	
2	$M^{-\cdot}$	315	−190.2	5.3	5.3
3	$[M-HF]^{-\cdot}$	295	−217.5	−22.0	−27.3
6	$[M-R]^-$	224	−176.8	18.8	13.5

All calculations were performed by the PM3 method as described in the Experimental section. The heat of formation for each species is for its most stable configuration. The overall heat of reaction is that for the reaction starting from the initial precursor, **1**, and having progressed to the current stage. The stepwise heat of reaction refers to that for the immediate mechanistic step (Schemes 2 and 3).

The heats of formation of neutral fragments used in the calculation of the relative and stepwise heats of formation were also calculated by the PM3 method: ΔH_f^0(HF) = −62.7, ΔH_f^0(HCN) = 33.0, ΔH_f^0 (NO) = 14.7, ΔH_f^0(C_6H_5CN) = 58.5, ΔH_f^0($C_6H_5CH{=}NH$) = 42.5, ΔH_f^0($C_6H_5CH_2CH$) = 52.1, and ΔH_f^0($C_6H_5CH_2CH{=}NH$) = 37.7 kcal mol^{-1}.

The species numbers correspond to the labels for structures or the corresponding anti-isomers in Schemes 2 and 3. The calculations involving the anti-isomers were performed on principal ions that preserve isomeric stereochemistry.

Table 5
Accurate mass measurements of fragment ions from the radical anions of the PFBO derivatives of aldehydes

Aldehyde	Elemental composition	Measure mass	Calculated mass	Deviation (ppm)	[a]Ion assignment
p-hydroxyphenyl-acetaldehyde	$C_{15}H_9NO_2F_4$	311.0656	311.0569	1.10	$[M-HF]^{-\cdot}$
	$C_{14}H_8O_2F_4$	284.0485	284.0460	−0.80	$[M-HF-HCN]^{-\cdot}$
Phenylacetaldehyde	$C_{15}H_9NOF_4$	295.0604	295.0620	5.50	$[M-HF]^{-\cdot}$
	$C_{14}H_8OF_4$	268.0522	268.0511	−5.10	$[M-HF-HCN]^{-\cdot}$
	$C_{15}H_9F_4$	265.0630	265.0640	3.90	$[M-HF-NO]^{-}$
Acrolein	$C_{10}H_5NOF_4$	231.0301	231.0307	2.60	$[M-HF]^{-\cdot}$
	$C_{10}H_5F_4$	201.0327	201.0331	2.00	$[M-HF-NO]^{-}$
Common fragment ions	$C_8H_2NOF_4$	204.0069	204.0072	1.60	$[M-HF-R]^{-}$
	$C_7H_2OF_5$	197.0047	197.0026	−4.70	
	$C_7H_2F_5$	181.0077	181.0076	−0.40	
	$C_7H_2OF_4$	178.0043	178.0042	−0.90	$[M-HF-RCN]^{-\cdot}$

[a]R refers to base group in the aldehyde R–CHO.

classes as summarized in Table 2; all but four ratios were less than 1.5, which we consider insignificant, given the variability between spectra. We found that A_{syn}/A_{anti} is 8.5 for $M^{-\cdot}$ and 30 for $[M - HF - HCN]^{-\cdot}$ ions; in addition, A_{syn}/A_{anti} is 3.7 for $[M - 181]^{-}$ and A_{anti}/A_{syn} is 3.0 for m/z 204 ions. The strong preference for the syn isomer to form an $M^{-\cdot}$ ion and/or allow its persistence implies that stereochemical constraints are involved in the production and/or stability of the $M^{-\cdot}$ ion. Likewise, the strong preference of the syn isomer in producing the $[M - HF - HCN]^{-\cdot}$ ion implies a mechanistic pathway where configurations derived from the original stereochemistry are preserved.

We propose that the initial formed molecular anion, $M^{-\cdot}$, (**1**; in Schemes 2 and 3) cyclizes to a structure that features a six-membered ring and yet maintains isomeric identity (**2** in Schemes 2 and 3) and that all rearrangement-based fragmentations of $M^{-\cdot}$ proceed through this cyclic form. The formation of this cyclic intermediate does not require a large investment of energy; the *anti*- and *syn*-PFBO-benzaldehyde anions require 6.3 and 7.9 kcal mol^{-1}. Additional investments of 17.2 and 12.1 kcal mol^{-1}, respectively, are required to surmount the transition state connecting **1** and **2**.

The molecular anion, $M^{-\cdot}$, is not only more abundant for the syn isomers but also is not uniformly detectable in the EC mass spectra of the PFBO-derivative of aldehydes (Table 1). However, elimination of HF from the molecular anion yields an $[M–20]^{-\cdot}$ ion, a major fragment ion for most derivatives (Table 1). The formula of this putative $[M - HF]^{-\cdot}$ ion was verified by accurate-mass measurement (Table 5). Furthermore, production of this ion shows no preference for anti or syn isomers, a fact that is observed for all other fragment ions except those previously noted.

The origin of the H in the HF loss was explored with the PFBO-derivative of d_8-phenylacetaldehyde; the molecular anion eliminates DF rather than HF (data not shown), indicating that the H in the departing HF does not arise from the benzylic methylene group of the derivatizing moiety. It was previously reported that the molecular anion of the PFBO-derivative of ring-labeled 2,3,4,5,6-pentadeuterobenzaldehyde loses HF, not DF [11], indicating that the source of H is not the aromatic ring of the derivatized benzaldehyde. The origin of the H in the HF loss must be the N=CH moiety, where the CH is from the aldehyde function, R–CHO. We postulate that HF loss occurs from the cyclic form of $M^{-\cdot}$, **2**, and leads to the formation of the intermediate **3**, also having a six-membered ring, as illustrated in Scheme 2. A similar intermediate can also be used to rationalize the EC mass spectra of fluoroacyl derivatives of catechols and 2-hydroxyaniline compounds [23].

The formation of the sterically favorable six-

membered ring configuration with an extended conjugated structure is highly exothermic, both overall and stepwise. Furthermore, the conjugated structure would extend through the aldehyde portion in cases when the carbonyl group is conjugated with an aromatic or olefinic group. The stability conferred by conjugation accounts for the high abundance of the $[M - HF]^{-\cdot}$ ion from acrolein, benzaldehyde, and possibly the aldehydes derived from Tyr and Trp (Table 1). We further propose that the six-membered ring intermediate, **3**, decomposes to yield the other major fragment ions as summarized in Scheme 2. The proposed structures of the ions and the mechanisms of formation are supported by data obtained by linked-scanning experiments and by CAD spectra from tandem mass spectrometry (data not shown).

The lack of isomeric preference in the formation of the $[M - HF]^{-\cdot}$ ion, **3**, implies that it is a common product for both syn and anti isomers and suggests that its mechanistic trajectory from **1** through **2** is equally facile for both isomers. Nevertheless, the syn isomer preferentially produces $M^{-\cdot}$ ions (**1** and **2**), and this may be understood by noting that $M^{-\cdot}$ is a minor ion whereas $[M - HF]^{-\cdot}$ is usually a major ion. Thus, small differences in rates of decomposition of the isomers would not significantly affect the abundance of the $[M - HF]^{-\cdot}$ ion but would have a profound influence on the persistence of the $M^{-\cdot}$ ions. In addition, the depletion of $M^{-\cdot}$ in the production of $[M - HF - HCN]^{-\cdot}$ and *m*/*z* 204 ions that favor the syn and anti isomers, respectively, would also affect the $M^{-\cdot}$ abundance.

Decomposition of the $[M - HF]^{-\cdot}$ ion results in formation of $[M - 40]^{-\cdot}$, $[M - 47]^{-\cdot}$, and $[M - 50]^{-}$ ions by losses of HF, HCN, and NO, respectively. Other common fragment ions, although not necessarily derived from the decomposition of $[M - HF]^{-\cdot}$, occur at *m*/*z* 204, 196, 178, and 162. The formulas of the ions, $[M - HF]^{-\cdot}$, $[M - HF - HCN]^{-\cdot}$, $[M - HF - NO]^{-}$, *m*/*z* 204, and *m*/*z* 178 were confirmed by accurate mass measurements (Table 5). The virtual lack of ions at $[M - 27]^{-\cdot}$ and $[M - 30]^{-}$ in the EC mass spectra indicates that the formation of $[M - HF - HCN]^{-\cdot}$ and $[M - HF - NO]^{-}$ ions is primarily through the $[M - HF]^{-\cdot}$ species. The routes of formation of these ions, except those for the *m*/*z* 162 and $[M - 2(HF)]^{-\cdot}$ ions, which usually arise by collisional activation, are rationalized in Schemes 2 and 3.

The proposed production of $[M - HF - NO]^{-}$ from $[M - HF]^{-\cdot}$, **3**, involves the breaking of the CO bond to form **3a**, an $[M - HF]^{-\cdot}$ ion, followed by the loss of $NO^{-\cdot}$ and cyclization, which are likely concerted, to form the product ion, **3z**. The calculated overall heat of reaction (Table 4) shows that the proposed route is endothermic, but is within the bounds of available energy, although the calculated energetics may present a pessimistic estimate in this case. Structure **3z** is the lowest energy form ion that we found among other reasonable candidates for an $[M - HF - NO]^{-}$ ion.

The route leading to elimination of NO from $[M - HF]^{-\cdot}$ must not be demanding because the $[M - HF - NO]^{-}$ fragment ion is produced from nearly all PFBO-aldehydes (Table 1) and is most abundant from PFBO-benzaldehyde and -acrolein. An $[M - 50]^{-}$ ion was also observed in the EC mass spectra of PFBO derivatives of other carbonyl-containing compounds [10–14]. Formation of this ion was previously attributed to the elimination of HF and of formaldehyde (HCHO) from the molecular anion of such compounds [12,13]. Not only would that cleavage require unlikely rearrangements, but also its formula does not agree with that established by accurate mass measurements. Instead the $[M - 50]^{-}$ ion is $[M - HF - NO]^{-}$ (Table 5).

We propose the route from **3** to the *m*/*z* 178 ion involves a 1,5 (or 1,3) H shift to form ion **4**, a transient $[M - HF]^{-\cdot}$ species that exothermically decomposes by a *retro* Diels–Alder reaction to produce the *m*/*z* 178 ion, **4z**, and benzonitrile in this case. Calculations show that the transition state for the *retro* Diels–Alder (*r*DA) reaction requires only 2.7 kcal mol^{-1} above that of the reactant **4**. Thus one expects the *r*DA to be a very facile decomposition accounting for the high abundance of the *m*/*z* 178. The proposed structure of the *m*/*z* 178 ion is discussed along with other candidates in a later section.

The large preference for the formation of $[M - HF - HCN]^{-\cdot}$ ions from the syn rather than the anti isomer strongly indicates that formation must proceed from structure **1** through an intermediate other than

3: one that would preserve stereochemical features traceable to the original isomers. We see that the configuration of the syn isomer of $M^{-\cdot}$, **2**, has an appropriate orientation for a 1,3 elimination of HF whereas the anti-derived configuration does not. Thus, we propose that the pathway for elimination of HCN (Scheme 3) starts with the elimination of HF from **2** to yield **7**, which then undergoes sequential addition-elimination through ion **7a**, to yield an $[M - HF]^{-\cdot}$ ion, **7b** has a seven-membered ring and is likely a minor component of the total population of $[M - HF]^{-\cdot}$ ions. Overall, the path from **1** to **7b** is essentially thermoneutral, but formation of **7** and **7a** requires some energy investment (Table 4). Furthermore, the transition states for **7** to **7a** and **7a** to **7b** require an additional 18.3 and 6.5 kcal mol^{-1}, respectively, above the energy of **7a**. This energy should be available from the ionization process (see the earlier discussion on simple fragmentations).

The ion **7b** possesses a contiguous HCN moiety that can be eliminated exothermically to form the $[M - HF - HCN]^{-\cdot}$ ion, **7z**. The theoretical calculation of likely reaction routes from **7b** to the final product, **7z**, suggests that the most likely reaction trajectory involves the sequential breaking of the weak NO bond and the weakened CC bond, liberating HCN followed by the formation of a CO bond to give **7z**.

CAD of the $[M - HF]^{-\cdot}$ ion derived from the PFBO derivative of phenylacetaldehyde produced the $[M - 2(HF)]^{-\cdot}$, $[M - HF - HCNO]^{-\cdot}$, $[M - HF - NO]^{-}$ ions and ions of *m*/*z* 178, 162, and 136 [Fig. 4(A)]. CAD of the $[M - DF]^{-\cdot}$ ion derived from the PFBO derivative of d_8-phenylacetaldehyde produced the $[M - 2(DF)]^{-\cdot}$, $[M - DF - DCNO]^{-\cdot}$, $[M - DF - NO]^{-}$ ions and ions of *m*/*z* 178, 162, and 136 [Fig. 4(B)]. The virtual absence of $[M - HF - HCN]^{-\cdot}$ or $[M - DF - DCN]^{-\cdot}$ ions produced from the $[M - HF]^{-\cdot}$ or $[M - DF]^{-\cdot}$ ions, respectively, indicates that the precursor $[M - HF]^{-\cdot}$ species for $[M - HF - HCN]^{-\cdot}$ production is indeed a minor component among all the $[M - HF]^{-\cdot}$ ions. The observation of ions of *m*/*z* 178, 162, and 136 for both cases indicates that these ions result from the loss of all remnants of the benzyl group of phenylacetaldehyde, also consistent with Scheme 2 and 3.

The fragment ion of *m*/*z* 204 is formed from the molecular anion of most PFBO-aldehydes (Table 1) and is the most abundant fragment produced from the molecular anion of PFBO derivative of MDA, a symmetrical dialdehyde. The formula of this ion, as determined by accurate-mass measurements, is consistent with the CAD spectra, which are invariant with regard to source molecular anions of the PFBO aldehydes (data not shown). Because the fractional abundance of this ion favors the anti-isomer, it must arise from preferential elimination of the R group ($C_6H_5CH_2-$) from the anti isomer of **2** to form a transient species **6** which in turn loses HF to form an unstable product, **6x**. The latter product ion rearranges to **6z**, the *m*/*z* 204 ion (Scheme 3).

We initially thought the ion at *m*/*z* 196 arose from a H· transfer accompanying the simple cleavage that otherwise produced the ion of *m*/*z* 197. However, the production of the *m*/*z* 196 ion from the molecular anion would be highly exothermic (Table 3) and should dominate the EC mass spectra. Moreover, the production of the complementary $[M - 196]^{-\cdot}$ ion would also be exothermic, yet, it is not observed, whereas the complementary pair of products, the *m*/*z* 181 and $[M - 181]^{-}$ ions, whose formation would be endothermic, do occur.

We propose that the route to formation starts with a 1,3-proton transfer in the cyclic $M^{-\cdot}$ species, **2**, to give **5**. Part of the driving force for this step is the elimination of hypovalent sites within **2**. The steps that follow involve the breaking of the weak NO bond to form the intermediate, **5a**, followed by the elimination of the aldehyde imine to give the *m*/*z* 196 ion, **5z** (2,3,4,5,6-pentafluorobenzaldehyde anion); these steps are calculated to be exothermic from ion **2** of both PFBO-benzaldehyde and PFBO-phenylacetaldehyde (Table 4). Furthermore, calculation of possible reaction paths indicates that the proposed route is energetically the most facile; the NO cleavage has essentially no barrier, and the transition state from **5a** to **5z** requires an activation energy of 12.7 kcal mol^{-1} above **5a** to surmount. The proposed mechanism for the generation of the *m*/*z* 196 ion also explains the absence of an $[M - 196]^{-\cdot}$ ion as seen in the EC mass spectra.

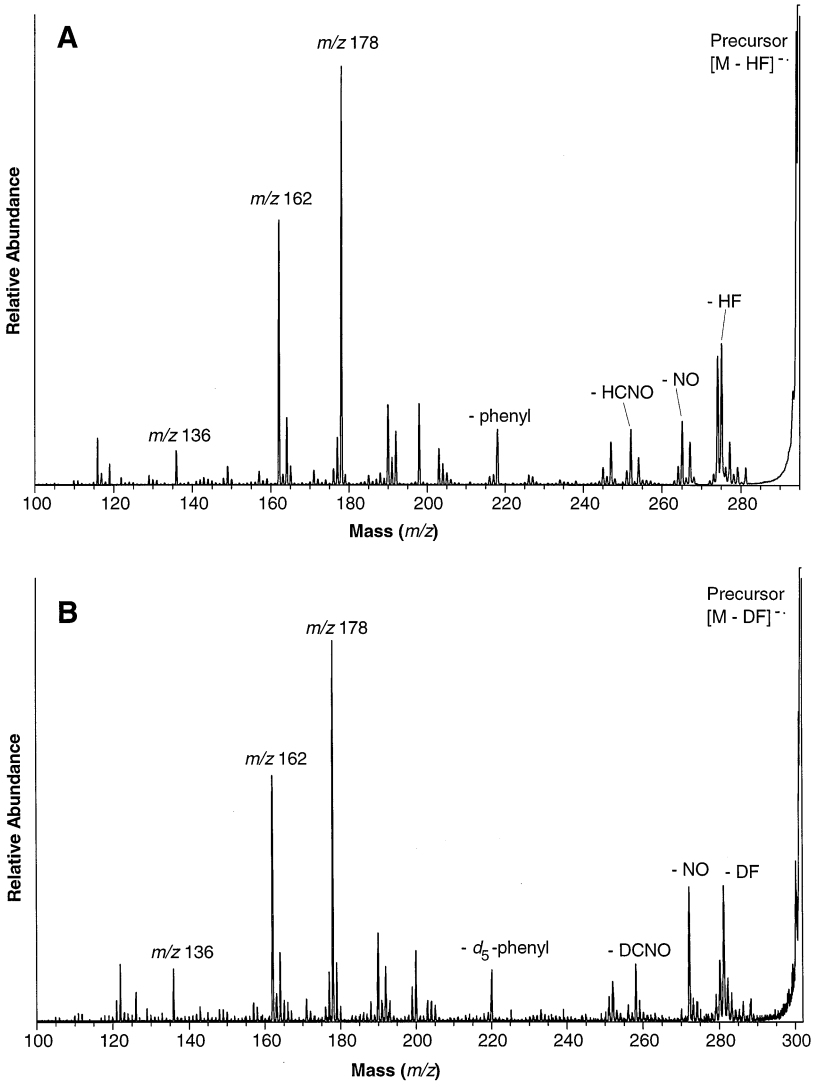

Fig. 4. The product ion CAD spectra of (A) the $[M - HF]^{-\cdot}$ ion of m/z 295 from PFBO-phenylacetylaldehyde and (B) the $[M - DF]^{-\cdot}$ ion of m/z 302 from PFBO-d_8-phenylacetylaldehyde obtained by tandem mass spectrometry.

3.3. The structure of m/z 178

The ion of m/z 178 is observed in all of the EC mass spectra (Table 1) and corresponds to the base peak in many of the spectra. CAD of the $[M - HF]^{-\cdot}$ ions yields an abundant fragment ion at m/z 178 (Fig. 4). Furthermore, precursor-ion scans obtained by B^2/E scanning confirm that the ion at m/z 178 arises from the $[M - HF]^{-\cdot}$ ion (data not shown). We propose that this ion is formed as depicted in Scheme 2 and discussed earlier. However, there are several possible isomers of the m/z 178 ion.

We calculated the relative heats of formation by both PM3 and ab initio methods (Experimental, Sec. 2.4) for six possible isomers of m/z 178, $C_7H_2OF_4^{-\cdot}$ (see Table 6 and accompanying drawings of the isomers). The isomers can be divided into two classes, low-energy (**A** and **B**) and high-energy (**C**

Table 6
Calculated relative energies of various isomers of *m*/*z* 178, $C_7H_2OF_4^{-\cdot}$

Form	Calculated relative energies (kcal mol^{-1})	
	PM3	Ab initio
A	0.0	0.0
B	6.8	2.5
C	76.3	57.5
D	82.2	
E	73.6	
F	90.1	59.0

Form: isomer as illustrated in Diagrams 1 and 2. The semiempirical PM3 and ab initio calculations were performed as described in Sec. 2.4 (Experimental); the results presented are for the most stable conformations of each form only. Form **A** (2,3,4,5-tetrafluorobenzaldehyde anion) is used to set the zero on both the relative PM3 and ab initio scales for relative energy, which is the difference between the heat of formation for a given form, and that for Form **A**.

Low-Energy Forms

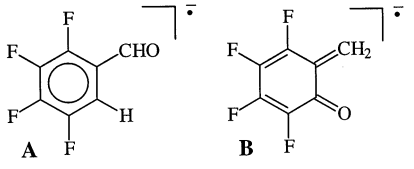

High-Energy Forms

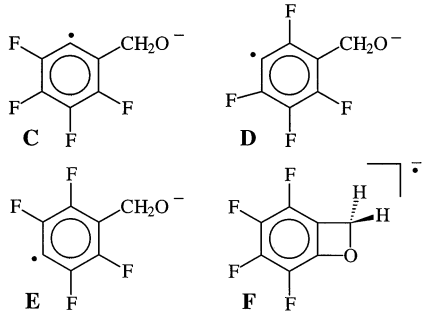

to **F**); the difference in heats of formation between the two classes is >50 kcal mol^{-1} and would make the production of **C** to **F** from **1** endothermic rather than exothermic by ~40 kcal mol^{-1} as it is for **A**. Furthermore, the production of **C** would require high-energy cleavages from **3**, compared to the facile *retro* Diels–Alder decomposition of **4** to form **A**. Furthermore, the production of **D** and **E** would require higher-energy forms of $[M - HF]^{-\cdot}$ ions as precursors. In addition, the route to **B** would be **C** → **F** → **B**, also involving the same energy investment as does the production of **C**. Thus, we propose that the *m*/*z* 178 ion is **A**, which is the most stable form of $C_7H_2OF_4^{-\cdot}$, as indicated by theoretical calculations, and has the most facile route of formation (Scheme 2).

4. Conclusion

The EC mass spectra of PFBO derivatives of aldehydes substituted with various R groups can be rationalized by a pair of schemes that class the products according to whether they arise from single bond cleavages (Scheme 1) of the molecular anion, $M^{-\cdot}$, or from fragmentation of intermediate products of rearrangements (Schemes 2 and 3). The second set arises from the cyclization of the molecular anion via a six-membered ring. That intermediate eliminates HF to form another, more stable intermediate which also has a six-membered ring; the H in the HF is derived from the embedded N=CH moiety. The first intermediate gives rise to product ions of $[M - HF - HCN]^{-\cdot}$ and *m*/*z* 204, which are isomerically specific, and the ion of *m*/*z* 196. The second intermediate produces all other major ions considered in this study. Among the latter group is an $[M - HF - NO]^-$ ion that is highly characteristic of PFBO-aldehydes.

The relative abundance of various product ions is determined in part by the negative charge dispersion and the degree of conjugation in the R group. Because reactive aldehydes are readily converted to PFBO derivatives and the PFBO group has high electron affinity, this derivative will be useful in the identification and detection of aldehydes in biological systems. An additional advantage is that the derivatization procedure is applicable to samples containing physiological concentrations of salt. Our preliminary GC/EC/MS studies demonstrate that many of the amino-acid-derived aldehydes generated by myeloperoxidase are present in human inflammatory tissues [24]. The mass spectrometric features we describe here provide a basis for understanding the GC/EC/MS spectra generated by the PFBO-aldehydes and for building a powerful tool to

investigate the role of reactive aldehydes in a wide range of physiological and pathological processes.

Acknowledgements

These studies were supported by U.S. Public Health Service grants R01-HL-62526, R01-AG-12293, R01-AG-15013, P01-DK-02456, and P41-RR-00954 and a grant from the American Heart Association.

References

[1] E. Schauenstein, H. Esterbauer, CIBA Found. Symp. 67 (1978) 225.
[2] E.R. Stadtman, Science 257 (1992) 1220.
[3] J.L. Witztum, D. Steinberg, J. Clin. Invest. 88 (1991) 1785.
[4] J.W. Baynes, Diabetes 40 (1991) 405.
[5] S.L. Hazen, J. Heller, F.F. Hsu, A. d'Avignon, J.W. Heinecke, Chem. Res. Toxicol., in press.
[6] M. Anderson, S.L. Hazen, F.-F. Hsu, J.W. Heinecke, J. Clin. Invest. 99 (1997) 424.
[7] S.L. Hazen, F.-F. Hsu, J.W. Heinecke, J. Biol. Chem. 271 (1996) 1861.
[8] S.L. Hazen, A. d'Avignon, M. Anderson, F.-F. Hsu, J.W. Heinecke, J. Biol. Chem. 273 (1998) 1997.
[9] S.L. Hazen, F.-F. Hsu, A. d'Avignon, and J.W. Heinecke, Biochemistry 37 (1998) 6864.
[10] A. Loidl-Stahlhofen, K. Hannemann, G. Spiteller, Chem. Phys. Lipids 77 (1995) 113.
[11] M.L. Selley, M.R. Bartlett, J.A. McGuiness, J.A. Hapel, N.G. Ardlie, M.J. Lacey, J. Chromatogr. 488 (1989) 329.
[12] X.P. Luo, M. Yazdanpanah, N. Bhooi, D.C. Lehotay, Anal. Biochem. 228 (1995) 294.
[13] D. de Boer, S.N. Bensink, A.R. Borggreve, R.D. van Ooijen, R.A.A. Maes, J. Mass Spectrom. 30 (1995) 497.
[14] D. de Boer, S.N. Bensink, A.R. Borggreve, R.D. van Ooijen, R.A.A. Maes, J. Mass Spectrom. 30 (1995) 505.
[15] A.D. Tait, D. Abbs, P. Teale, E. Houghton, Biomed. Environ. Mass Spectrom. 18 (1989) 572.
[16] J.J.P. Stewart, J. Comp. Chem. 10 (1989) 209.
[17] J.J.P. Stewart, J. Comp. Chem. 10 (1989) 221.
[18] M.J. Frisch, G.W. Trucks, H.B. Schlegel, P.M.W. Gill, B.G. Johnson, M.A. Robb, J.R. Cheeseman, T. Keith, G.A. Petersson, J.A. Montgomery, K. Raghavachari, M.A. Al-Laham, V.G. Zakrzewski, J.V. Ortiz, J.B. Foresman, J. Cioslowski, B.B. Stefanov, A. Nanayakkara, M. Challacombe, C.Y. Peng, P.Y. Ayala, W. Chen, M.W. Wong, J.L. Andres, E.S. Replogle, R. Gomperts, R.L. Martin, D.J. Fox, J.S. Binkley, D.J. Defrees, J. Baker, J.P. Stewart, M. Head-Gordon, C. Gonzalez, J.A. Pople, GAUSSIAN 94, Revision D.3, Gaussian, Inc., Pittsburgh, PA, 1995.
[19] M.J. Frisch, A. Frisch, J.B. Foresman, in GAUSSIAN 94, User's Reference, Gaussian, Inc., Pittsburgh, PA, 1995, and references therein.
[20] J.A. Pople, A.P. Scott, M.W. Wong, L. Radom, Israel J. Chem. 33 (1993) 345.
[21] A.D. Becke, J. Chem. Phys. 98 (1993) 5648.
[22] G.J. Karabatsos, N. Hsi, Tetrahedron 23 (1967) 1079.
[23] F.-F. Hsu, J. Turk, and M.L. Gross, submitted.
[24] F.F. Hsu, S.L. Hazen, J.W. Heinecke, unpublished observation.